Electrochemical Sensing toward Trace As(III) Based on Mesoporous MnFe$_2$O$_4$/Au Hybrid Nanospheres Modified Glass Carbon Electrode

Shaofeng Zhou [1,*]**, Xiaojuan Han** [1]**, Honglei Fan** [2] **and Yaqing Liu** [1,*]

[1]   Shanxi Province Key Laboratory of Functional Nanocomposites, North University of China,
    Taiyuan 030051, China; hanxj2015nn@163.com
[2]   Shanxi Province Key Laboratory of Higee-Oriented Chemical Engineering, North University of China,
    Taiyuan 030051, China; whutfanfan@163.com
*   Correspondence: zhoushaofeng@nuc.edu.cn (S.F.Z.); lyq@nuc.edu.cn (Y.Q.L.); Tel.: +86-351-3559669 (S.F.Z.)

Abstract: Au nanoparticles decorated mesoporous MnFe$_2$O$_4$ nanocrystal clusters (MnFe$_2$O$_4$/Au hybrid nanospheres) were used for the electrochemical sensing of As(III) by square wave anodic stripping voltammetry (SWASV). Modified on a cheap glass carbon electrode, these MnFe$_2$O$_4$/Au hybrid nanospheres show favorable sensitivity (0.315 µA/ppb) and limit of detection (LOD) (3.37 ppb) toward As(III) under the optimized conditions in 0.1 M NaAc-HAc (pH 5.0) by depositing for 150 s at the deposition potential of −0.9 V. No obvious interference from Cd(II) and Hg(II) was recognized during the detection of As(III). Additionally, the developed electrode displayed good reproducibility, stability, and repeatability, and offered potential practical applicability for electrochemical detection of As(III) in real water samples. The present work provides a potential method for the design of new and cheap sensors in the application of electrochemical determination toward trace As(III) and other toxic metal ions.

Keywords: arsenite; MnFe$_2$O$_4$/Au; electrochemical detection; SWASV

1. Introduction

Inorganic arsenic contamination in drinking water has become a serious worldwide threat to human health due to arsenic's high toxicity [1]. Such pollutants in drinking water may lead to many health problems, such as skin lesions, keratosis, lung cancer, and bladder cancer [2]. According to reports for twenty countries, the arsenic levels in drinking water is higher than the World Health Organization (WHO)'s arsenic guideline value of 10 µg·L^{-1} (*i.e.*, 10 ppb) [3,4]. Thus, it is rather important to have an accurate, rapid, and sensitive method to detect and monitor the environmental pollution of drinking water. Although various spectroscopic methods are excellent for arsenic testing in labs, they are very expensive and not suitable for *in situ* analyses due to the lengthy and complex instruments required [5,6]. However, electrochemical methods, particularly stripping voltammetry analysis, have provided promising techniques that are available for the sensitive detection and quantification of arsenic due to their low cost, portability, and suitability for on-site analysis [7–9]. The electrochemical application and performance of an electrode depends to a large extent on the materials from which it has been made. For the electrochemical detection of arsenic, a large effort has been poured into electrode materials and the modification of electrode surfaces in an attempt to improve their analytical performance [7,10]. So far, Au has been shown to be a promising choice in the sensitive determination of arsenic due to its excellent electrocatalytic ability [11,12]. However, considering the potential obstacles associated with using a solid gold macroelectrode, such as high costs, rigorous control, and care of the quality of its surface, Au nanoparticle modified

electrodes have drawn extensive attention and bring a new area to the voltammetric detection of inorganic arsenic [3,13]. It was reported that the Au nanoparticle modified electrode can behave as random arrays of microelectrodes with the superiority of enhanced mass transfer, efficient catalysis, and a controllable microenvironment [14–16].

Recently, metal-oxide nanomaterials have been creatively introduced into voltammetric responses for inorganic arsenic due to their excellent catalytic activity and adsorption ability [17–19]. Fe_3O_4, as a low-cost, eco-friendly, and easily-prepared material with ideal catalytic and absorption activity, has attracted great attention for its high sensitivity and rapid response toward arsenic via the electrochemical method [7]. Gao reported using Fe_3O_4 microspheres composited with room-temperature ionic liquids (RTILs) for the determination of As(III), which reached an exciting electrochemical performance (sensitivity: 4.91 μA/ppb; LOD: 0.0008 ppb) for the detection of As(III) through square wave anodic stripping voltammetry (SWASV) compared with the noble-metal nanoparticle modified electrodes [18]. Monodispersed Fe_3O_4 nanocrystals were also reported that could be exploited in order to remove arsenic from water due to their strong adsorption capacity [20]. To enhance the electrochemical behavior of Fe oxides toward arsenic, it was found that the addition of another metallic element not only changed the surface characteristics and micro-structure of the Fe oxide, but also participated in the process of arsenic removal [21]. Noteworthy, MnO_2 plays a role as an oxidant in the As(III) uptake by FMBO and MNFHO, which could perform much better than pure Fe oxides for the removal of As(III). [22,23]. Xu *et al.* reported the $MnFe_2O_4$ combined with uniform mesoporous structured and small constituent nanocrystals can provide a synergistic effect for the enhanced adsorption performance toward As(III) [24]. After being modified on a gold electrode, the Mn doped mesoporous $MnFe_2O_4$ nanocrystal clusters exhibited favorable sensing behavior toward As(III) with the sensitivity of 0.295 μA/ppb and LOD of 1.95 ppb by SWASV [25]. Thus, it is inferred that doping Mn oxides could provide a synergistic effect with Fe and Mn species for As(III) removal or detection contributed to the higher electrochemical reactivity.

In this work, considering the high electrochemical response of Mn doped iron oxide and the excellent electrocatalytical ability of Au nanoparticles towards As(III), we have explored Au nanoparticle decorated mesoporous $MnFe_2O_4$ nanocrystal clusters ($MnFe_2O_4$/Au hybrid nanospheres) for electrochemical sensing of As(III) by square wave anodic stripping voltammetry (SWASV) [26,27]. A glass carbon electrode (GCE) was chosen as the base electrode in order to further reduce the cost. The structure and synergistic effect of the $MnFe_2O_4$/Au hybrid nanospheres were characterized and studied. The optimization of detection conditions—including considerations regarding supporting electrolytes, pH values, deposition potentials, and deposition times—were investigated. Moreover, electrochemical interference behavior, reproducibility, stability, repeatability, and real sample analysis of the $MnFe_2O_4$/Au hybrid nanospheres modified GCE were also studied in detail under the optimum experimental conditions.

2. Materials and Methods

2.1. Chemical Reagents

All chemicals were analytical grade, and were commercially available from Shanghai Chemical Reagent Co. Ltd without further purification. Acetate buffer solutions of 0.1 M at different pH values were prepared by mixing stock solutions of 0.1 M NaAc, HAc, and NaOH. Phosphate buffer solutions (PBS) of 0.1 M were prepared by mixing stock solutions of 0.1 M H_3PO_4, KH_2PO_4, K_2HPO_4, and NaOH. NH_4Cl-$NH_3 \cdot H_2O$ (0.1 M) solutions were prepared by mixing stock solutions of 0.1 MNH_4Cl and $NH_3 \cdot H_2O$ in different proportions. All stock and working solutions were prepared in purified water (18.2 MΩ cm), which was obtained through a GWA-UN to Pure & Ultrapure water purification system (Purkinje General).

2.2. Apparatus

The Electrochemical measurements were performed on a CHI 660E computer-controlled potentiostat (ChenHua Instruments Co., Shanghai, China). A conventional three-electrode configuration was employed, consisting of a bare or modified glass carbon electrode (GCE) as a working electrode, an Ag/AgCl/saturated KCl electrode as a reference electrode, and a platinum wire as a counter electrode. Scanning electron microscopy (SEM) observation and energy-dispersive X-ray spectrum (EDS) analyses were carried out on a Quanta 200 FEG scanning electron microscope (FEI Company, Hillsboro, OR, USA). The High Resolution Transmission Electron Microscopy (HRTEM) and Transmission Electron Microscopy (TEM) images analyses were carried out on JEM-2010 and JEM-1400 microscopes (JEOL, Tokyo, Japan), respectively.

2.3. Preparation of Mesoporous MnFe₂O₄/Au Hybrid Nanospheres

Firstly, the mesoporous $MnFe_2O_4$ nanocrystal clusters ($MnFe_2O_4$ NCs (nanocrystal clusters)) were prepared according to a previous report [28]. Then they were APTMS-functionalized according to the previous report with some modification showing as follow [29]: $MnFe_2O_4$ NCs (20 mg) were added to a solution containing ethanol (30 mL) and water (2 mL), followed by the addition of ammonium hydroxide (25%; 2 mL) and APTMS (200 μL). Then, the resulting solution was sonicated continuously for about 8 h. After four-step separation by means of an external magnetic field, the resulting APTMS-functionalized $MnFe_2O_4$ NCs was dissolved in water (10 mL). After being selected with a magnet and rinsed with water four times, the resulting APTMS-functionalized $MnFe_2O_4$ NCs were dissolved in water (10 mL) for further use.

Subsequently, the solution of APTMS-functionalized $MnFe_2O_4$ NCs (1 mL) was mixed with 20 mL solution of Au nanoparticles via shaking for 24 h. The solution of Au nanoparticles was synthesized according to previously described methods [30]. The resulting product of mesoporous $MnFe_2O_4$/Au hybrid nanospheres was collected through an external magnet. An illustration of the preparation procedure of mesoporous $MnFe_2O_4$/Au hybrid nanospheres can be followed in Scheme 1.
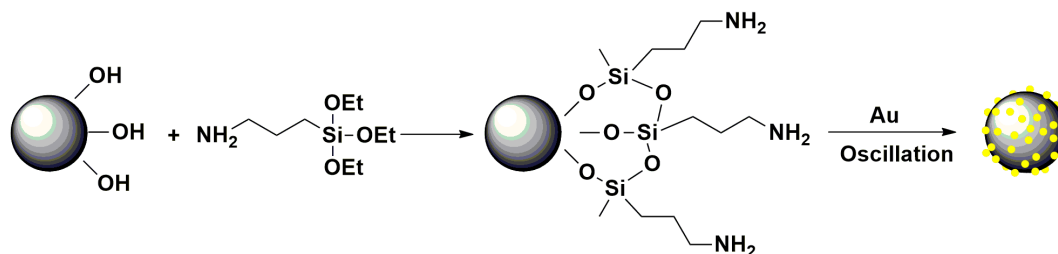
Scheme 1. Illustration of the preparation of mesoporous $MnFe_2O_4$/Au hybrid nanospheres.

2.4. Preparation of Mesoporous MnFe₂O₄/Au Hybrid Nanospheres Modified GCE

Firstly, the GCE was polished with 0.3 μm and 0.05 μm alumina power slurries sequentially to form a mirror-shiny surface. Next, it was sonicated with 1:1 HNO_3 solution, absolute ethanol, and water for 1 min, respectively. Subsequently, the mesoporous $MnFe_2O_4$/Au hybrid nanospheres film on the surface of the GCE was produced as follows: Mesoporous $MnFe_2O_4$/Au hybrid nanospheres (2 mg) were dispersed into purified water (2 mL) to obtain a uniform dispersion by 3 min of sonication. A drop of the above $MnFe_2O_4$/Au hybrid nanospheres solution was pipetted onto the fresh surface of the GCE and dried in air. After evaporation, a thin mesoporous $MnFe_2O_4$/Au hybrid nanospheres film was formed on the surface of the GCE.

2.5. Electrochemical Measurements

The electrochemical behavior for the $MnFe_2O_4$/Au hybrid nanospheres modified GCE was observed through square wave anodic stripping voltammetry (SWASV) under the optimized conditions.

Under the potential of −0.9 V for 150 s, As(0) was deposited by the reduction of As(III) in 0.1 M HAc-NaAc (pH 5.0). Subsequently, the electrodeposited As(0) was anodic stripped to As(III) which was performed in the potential range of −0.4 to 0.4 V under the following conditions: frequency, 25 Hz; amplitude, 25 mV; increment potential, 4 mV; *vs.* Ag/AgCl. Thereafter, desorption potential of −0.9 V for 150 s was carried out to remove the residual As(0) under stirring conditions. The same experimental conditions were applied in the interference, reproducibility, stability, repeatability, and real sample analysis studies. Cyclic voltammograms (CV) and electrochemical impedance spectra (EIS) were performed in the mixing solution containing 5 mM $Fe(CN)_6^{3-/4-}$ and 0.1M KCl with the scanning rate of 100 mV·s^{-1}.

3. Results and Discussion

3.1. Characterization of Mesoporous MnFe₂O₄/Au Hybrid Nanospheres

Figure 1a–c show the as-prepared mesoporous $MnFe_2O_4$ sample is made up of monodisperse, uniform, and smooth-faced microspheres with diameters of about 350 nm. The HRTEM image indicates that the individual microsphere contains lots of loose clusters, which are composed of primary nanocrystals with the size of about 8–12 nm (Figure 1b). This mesoporous architecture might provide the microspheres with large surface areas in favor of adsorbing guest molecules [31–33]. The selected-area electron diffraction (SAED) pattern indicates that the diffraction spots are widened into narrow arcs (insets of Figure 1b), also signifying the clusters are composed of many misaligned ferrite nanocrystals [31,34]. The d value of the crystal plane (311) shown in Figure 1c verifies the crystalline structure of $MnFe_2O_4$ NCs. Taking the analyses of SEM and HRTEM mentioned above, $MnFe_2O_4$ NCs with diameters of 350 nm and mesoporous structures composed of nanocrystals with the size of about 11 nm have been prepared successfully, which might render them with large surface areas in favor of adsorbing and detecting heavy metal ions. Figure 1d,e show the SEM and TEM images of mesoporous $MnFe_2O_4$/Au hybrid nanospheres. The corresponding images show that 13 nm Au nanoparticles (insets of Figure 1e) are decorated on the surface of mesoporous $MnFe_2O_4$ microspheres. The hybrid nanospheres with rough surfaces decorated by Au nanoparticles are able to combine the good catalytic activity of Au and high adsorption activity of mesoporous $MnFe_2O_4$ toward heavy metal ions simultaneously, thus it might offer good electrochemical activity for detection toward trace As(III).

3.2. Electrochemical Characterization of Mesoporous MnFe₂O₄/Au Hybrid Nanospheres Modified GCE

The typical cyclic voltammetry (CV) of bare GCE, Au, $MnFe_2O_4$ NCs, and $MnFe_2O_4$/Au hybrid nanospheres modified GCE were electrochemically characterized in a solution of 5 mM $Fe(CN)_6^{3-/4-}$ with 0.1 M KCl (Figure 2a). Both the bare and modified GCE were observed to exhibit a pair of well-defined reversible redox peaks. Compared with the bare GCE, Figure 2a displays the anodic and cathodic peak currents for Au, $MnFe_2O_4$ NCs, and $MnFe_2O_4$/Au hybrid nanospheres modified GCE which all decline apparently, which thereby indicates that the bare GCE has been modified successfully by the above nanomaterials. Among all the modified GCE, it can be found that the anodic and cathodic peak currents of the $MnFe_2O_4$ NCs modified GCE is the lowest, which is due to the poor conductivity of the metal oxide on the surface of the bare GCE which can slow the electron transfer [35]. However, after being decorated by Au nanoparticles, the anodic and cathodic peak currents of $MnFe_2O_4$/Au hybrid nanospheres modified GCE observably increases and the peak-to-peak separation (△Ep) decreases from 190 mV to 120 mV, indicating the electron transfer of $MnFe_2O_4$ NCs were improved observably by the hybrid of the Au nanoparticles on the surface of $MnFe_2O_4$ NCs.
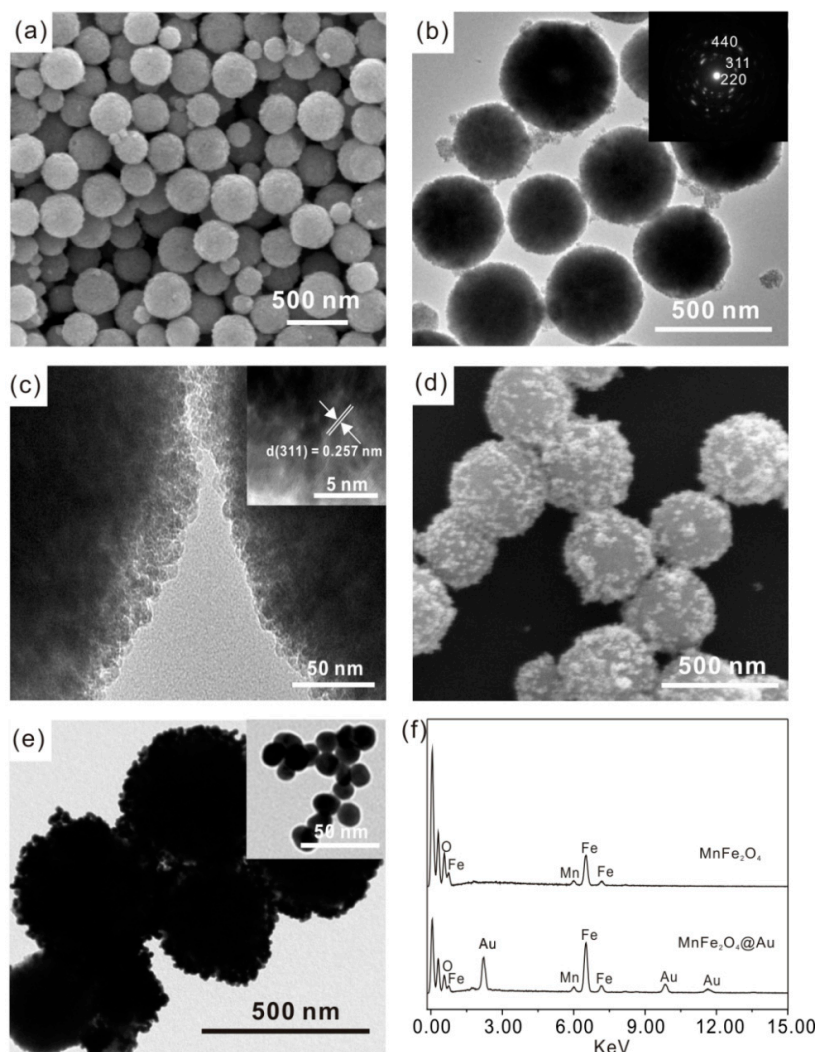
Figure 1. Characterization of mesoporous $MnFe_2O_4$/Au hybrid nanospheres: (**a**) Scanning electron microscopy (SEM) image of $MnFe_2O_4$ NCs; (**b**) and (**c**) The High Resolution Transmission Electron Microscopy (HRTEM) images of $MnFe_2O_4$ NCs, inset in panel b is the corresponding selected-area electron diffraction (SAED) pattern; (**d**) SEM image of $MnFe_2O_4$/Au hybrid nanospheres; (**e**) TEM image of $MnFe_2O_4$/Au hybrid nanospheres, inset in panel e is the TEM image of Au nanoparticle decorated on the surface of $MnFe_2O_4$ NCs; (**f**) Energy-dispersive X-ray spectrum (EDS) of $MnFe_2O_4$ NCs and $MnFe_2O_4$/Au hybrid nanospheres.

The interface properties of the bare GCE, Au, $MnFe_2O_4$ NCs, and $MnFe_2O_4$/Au hybrid nanospheres modified GCE are further analyzed by electrochemical impedance spectroscopy (EIS). The diameter of the semicircle equals the electron transfer resistance (R_{et}), and the R_{et} controls the electron transfer kinetics of the redox probe at the surface of the electrode. Figure 2b shows the EIS of bare GCE displays an almost straight line, implying the bare GCE conducts electricity very well. In addition, there is a small semicircle domain for the EIS of Au nanoparticles modified GCE, thereby meaning a very low R_{et} for this modified electrode. However, Figure 2b shows the R_{et} of the $MnFe_2O_4$ NCs modified GCE was much higher than the bare or Au nanoparticles modified GCE, indicating that the $MnFe_2O_4$ NCs layer blocked the electron transfer of the electrochemical probe. Due to the poor conductivity of metal oxide, the modification of $MnFe_2O_4$ NCs could further pose a barrier and hinder the access of the redox probe to the electrode surface, thus resulting in a large R_{et} of the $MnFe_2O_4$ NCs modified GCE. Interestingly, the EIS of the $MnFe_2O_4$/Au hybrid nanospheres modified GCE shows a much smaller semicircle compared with the $MnFe_2O_4$ NCs modified GCE, indicating that the

decorating of Au nanoparticles on the surface of $MnFe_2O_4$ NCs could improve the electron transfer of $MnFe_2O_4$ NCs on the surface of the GCE, which is consistent with the above CV results.

Figure 2c presents the SWASV analytical results of the $MnFe_2O_4$ NCs, Au nanoparticles, and $MnFe_2O_4$/Au hybrid nanospheres modified GCE. When the accumulation process was performed for 150 s at −0.9 V in 50 ppb As(III) solution containing 0.1 M acetate buffer (pH 5.0), it shows no peak appears in the curve of the $MnFe_2O_4$ NCs modified GCE, and a weak peak at −0.9 V can be observed for the Au nanoparticles modified GCE. For the $MnFe_2O_4$/Au hybrid nanospheres modified GCE, the peak current increases much higher than the single $MnFe_2O_4$ NCs or Au nanoparticles modified GCE. It shows that the hybrid that consists of Au nanoparticles on the surface of $MnFe_2O_4$ NCs could provide much more remarkable electrochemical performances towards As(III) detection. It might be attributed to the catalytic effect and high electron transfer of Au nanoparticles would provide much more active sites for the electrochemical reactions in the detection process of As(III). Thus, based on the unique mesoporous structure of the $MnFe_2O_4$ NCs responses to As(III) [25], the hybrid of Au nanoparticles on the surface of $MnFe_2O_4$ NCs indeed provides a synergistic effect for the detection of As(III) through SWASV.
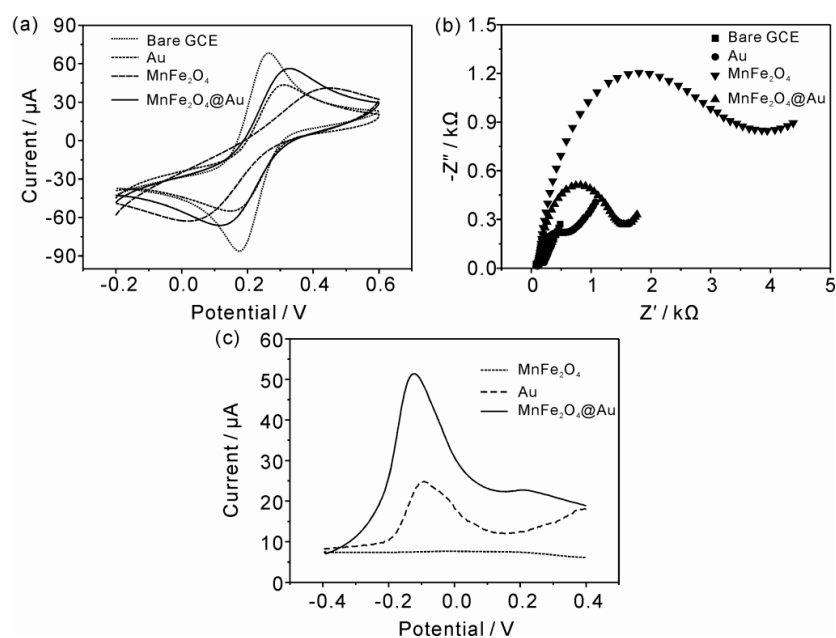

Figure 2. Cyclic voltammograms (**a**) and Nyquist diagram of electrochemical impedance spectra (**b**) for bare glass carbon electrode (GCE), Au nanoparticles (NPs), $MnFe_2O_4$ NCs, $MnFe_2O_4$/Au hybrid nanospheres modified GCE in the solution of 5 mM $Fe(CN)_6^{3-/4-}$ containing 0.1 M KCl. (**c**) SWASVs (square wave anodic stripping voltammetries) for 50 ppb As(III) on the $MnFe_2O_4$ NCs, Au NPs, $MnFe_2O_4$/Au hybrid nanospheres modified GCE in 0.1 M HAc-NaAc (pH 5.0). Deposition potential: −0.9 V, deposition time: 150 s, step potential: 4 mV, amplitude: 25 mV, frequency: 25 Hz, *vs.* Ag/AgCl.

3.3. Optimum Experimental Conditions of Electrochemical Detection of As(III)

The optimization of experimental conditions (supporting electrolytes, pH, deposition potential, and deposition time) was taken into account using SWASV. The effect of supporting electrolytes at pH 5.0 was tested and NaAc-HAc was finally chosen as the best electrolyte in comparison with PBS and NH_4Cl-NH_4OH (Figure 3a). The effect of pH on the SWASV response was investigated in the pH range of 3.0–8.0 in 0.1 M NaAc-HAc solutions, as shown in Figure 3b. The maximum peak current was achieved when the solution was maintained at pH 5.0. The decline of the pH value would provide a more acidic environment resulting in the destruction of mesoporous $MnFe_2O_4$ NCs, thus the stripping current became poor. The stripping current also observably declined when the pH value increased to a

high level, such as 7 or 8, which is consistent with the report that the adsorption capacity of As(III) decreased under higher pH values [36]. In a higher pH solution, the electrostatic attraction will weaken between the negatively charged As(III) species and positively charged surface sites of $MnFe_2O_4$ NCs. Thus, pH 5.0 was chosen for the preconcentration solution in this experiment. Different deposition potentials in the range of -1.2 to -0.4 V were also experimented with via SWASV by standard additions of 50 ppb As(III) in 0.1 M NaAc-HAc (pH 5.0), as shown in Figure 3c. It was found that the deposition potential negative shifts from -0.4 V to -0.9 V (*vs.* Ag/AgCl) can obviously improve the peak current of reduction of As(III). Generally, the peak current would reach a plateau, settling to a constant value which should be the optimum deposition potential. However, when the potentials beyond -0.9 V were applied, a decrease response of the peak current were observed, as shown in Figure 3c, due to the reduction of hydrogen, which would lead to the formation of micro gas bubbles and thus reduce the effective electrode area and weaken the response of As(III) [35]. Therefore, the deposition potential of -0.9 V was selected for further studies. The dependence of the stripping peak current of As(III) at the deposition time on the sensing response was studied under 50 ppb As(III) (pH 5.0). Figure 3d shows the stripping peak current improved with the deposition time increase from 30 s to 240 s. Although the sensitivity was improved under a longer deposition time, it also reduced the upper detection limit due to the surface saturation in the high metal ion concentration [37]. When the deposition time exceeded 150 s, the increased velocity of the stripping current become slower, suggesting that the electrode surface was approximately saturated by the As(III). Considering the time consumed, the optimized deposition time of 150 s was used throughout. At last, the optimum experimental conditions for the electrochemical detection of As(III) was determined in 0.1 M NaAc-HAc (pH 5.0) by depositing it for 150 s under the deposition potential of -0.9 V.
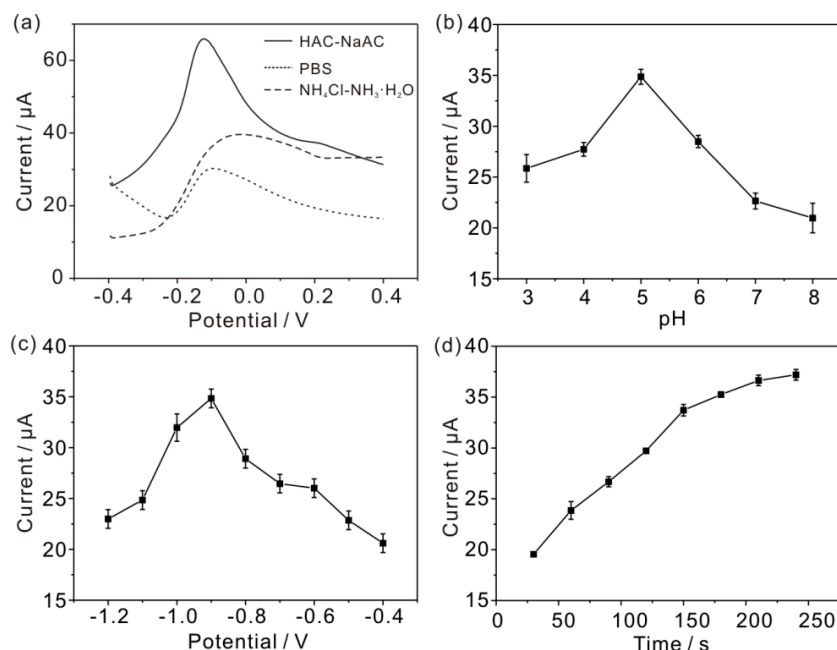

Figure 3. Influence of (**a**) supporting electrolytes; (**b**) pH value; (**c**) deposition potential; and (**d**) deposition time on the voltammetric response of the $MnFe_2O_4$/Au hybrid nanospheres modified GCE. Data were evaluated by SWASV of 50 ppb As(III).

3.4. Electrochemical Detection of As(III) with $MnFe_2O_4$/Au Hybrid Nanospheres Modified GCE

Under the optimal experimental conditions, As(III) was determined on the $MnFe_2O_4$/Au hybrid nanospheres modified GCE using SWASV. Figure 4a presents the SWASV response toward As(III) over the concentration ranges of 10 to 110 ppb. The linearization equation was $i/\mu A = 18.6 + 0.315\ c/ppb$, with the correlation coefficient of 0.996 (Figure 4b). Based on a signal-to-noise ratio equal to 3 (3σ

method), the theoretical limit of detection (LOD) was estimated to be 3.37 ppb. The sensitivity and LOD of this study were compared with other previously reported electrodes listed in Table 1. In contrast to other Au electrode systems, it can be observed that the proposed electrode can obtain preferable sensitivity (0.315 μA/ppb) while remaining cheap at the same time. Although the LOD of 3.37 ppb is high, it is still within the maximum permissible limits for As(III) in drinking water issued by the World Health Organization (10 ppb). However, compared with the Fe_3O_4-RTIL modified SPCE [18], the sensitivity and LOD of this proposed sensor was at a disadvantage. It was considered that the Fe_3O_4-RTIL composite could provide a specific interface for arsenic to accumulate and exchange electrons, thus future studies focusing on the $MnFe_2O_4$-Au-RTIL composite may obtain exciting sensitivity and LOD for the electrochemical sensing of As(III).
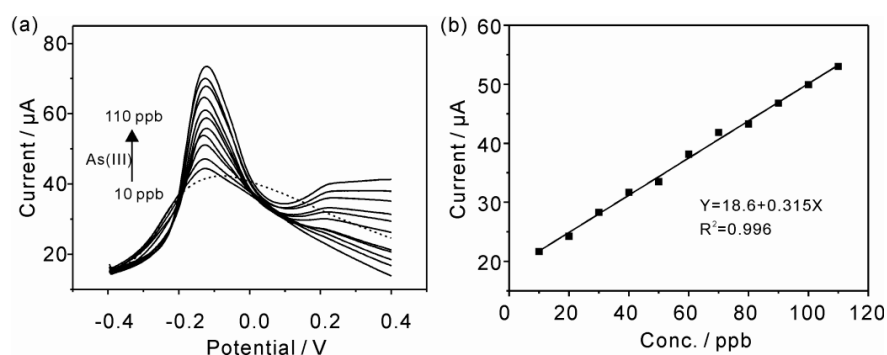

Figure 4. SWASV responses (**a**) and the corresponding calibration plot (**b**) of the $MnFe_2O_4$/Au hybrid nanospheres modified GCE toward As(III) over a concentration range of 10 to 110 ppb by depositing for 150 s in 0.1 M HAc-NaAc (pH 5.0). Deposition potential: −0.9V, step potential: 4 mV, amplitude: 25 mV, and frequency: 25 Hz.

Table 1. Comparison of current sensitivity with previously reported values of different electrodes for electrochemical detection of As(III).

Electrode	Sensitivity (μA/ppb)	LOD (ppb)	Refs.
Au-UMEA	0.044	0.013	[38]
Au NPs/GCE	0.24	0.0096	[3]
PBSPE	0.000387	1.875	[39]
Gold-carbon composite electrode	0.133	0.375	[40]
MWCNTs/gold electrode	0.236	-	[41]
Co_3Ox/GCE	0.00148	0.825	[17]
$MnFe_2O_4$/gold electrode	0.295	1.95	[25]
$MnFe_2O_4$/Au modified GCE	0.315	3.37	This work
Fe_3O_4-RTIL modified SPCE	4.91	8×10^{-4}	[18]

3.5. Interference Measurements

Commonly, the other metal ions can coprecipitate and strip off under the experimental conditions for determination of As(III), thus sensitive detection of As(III) in the real sample without interference is a challenging task. In order to investigate the interference of other heavy metal ions to the electrochemical determination of As(III), a series of interference measurements were studied. Figure 5 presents the SWASV response of $MnFe_2O_4$/Au hybrid nanospheres modified GCE in 0.1 M HAc-NaAc (pH 5.0) containing 50 ppb As(III) in the presence of Cd(II), Hg(II), Pb(II), and Cu(II) and over a concentration range of 0 to 500 ppb, respectively. Figure 5a,b show the peak stripping currents of As(III) almost stays the same as the concentrations of Cd(II) and Hg(II) increase linearly. When the concentrations of Cd(II) and Hg(II) are up to 10-fold the concentration of As(III), the peak current of As(III) still changes a little. It means Cd(II) and Hg(II) do not observably interfere with the detection of

As(III) for the MnFe$_2$O$_4$/Au hybrid nanospheres modified GCE when sensing the two target metal ions simultaneously. As to the interference of Cu(II), Figure 5c indicates the peak currents of As(III) also remain the same when the concentration of Cu(II) is less than 300 ppb. However, the peak current of As(III) drops observably when the concentration of Cu(II) increases further. Therefore, it means that Cu(II) would interfere with the detection of As(III) for the MnFe$_2$O$_4$/Au hybrid nanospheres modified GCE when the concentration of Cu(II) is beyond a certain value when the Cu(II) and As(III) coexist within a solution. On the other hand, Figure 5d shows that the peak current of As(III) almost rises linearly as the concentration of Pb(II) increases from 0 to 500 ppb. These results indicate that the existence of Pb(II) would enhance the detection signal of As(III) to some extent. This can be reasoned by the mutual promotion of adsorption sites between Pb(II) and As(III) before the adsorbing capacity of heavy metal ions reaches saturation.
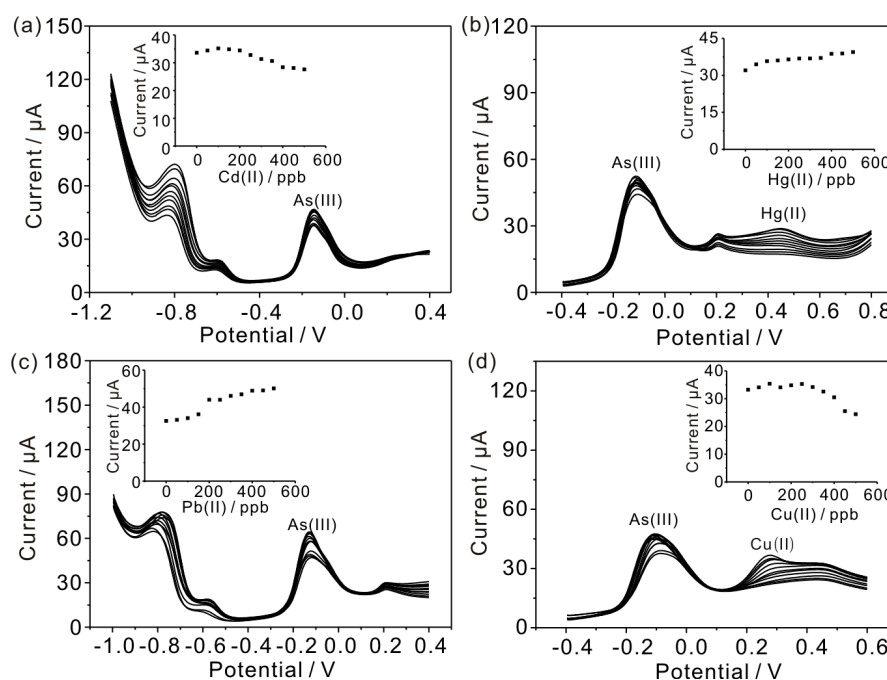

Figure 5. SWASV responses of the MnFe$_2$O$_4$/Au hybrid nanospheres modified GCE containing 50 ppb As(III) in the presence of Cd(II), Hg(II), Pb(II), and Cu(II) over a concentration range of 0 to 500 ppb, respectively. (Insets in panel a, b, c, and d are the corresponding peak currents toward 50 ppb As(III) over a concentration range of 0 to 500 ppb of interfering ions.) Electrochemical stripping conditions are identical to those in Figure 4.

3.6. Reproducibility, Stability and Repeatability

To evaluate the reproducibility of the modified electrode, six MnFe$_2$O$_4$/Au hybrid nanospheres modified GCEs were prepared following the same procedure and were applied to detect 50 ppb As(III) in 0.1 M HAc-NaAc (pH 5.0) under the optimized conditions. The relative standard deviation (RSD) derived from the peak currents from six tests was 3.9%, indicating that the developed method has good reproducibility. Additionally, the stability of the modified electrodes were investigated by storing six prepared electrode at 4 °C for ten days, and then testing the SWASV response toward 50 ppb As(III) under the optimized conditions. The result showed that the stripping peak current only decreased by 7.8%, 7.3%, 3.7%, 4.6%, 7.0%, and 4.8% of the first value, thereby showing a long-term stability of the fabricated electrode. Moreover, the repeatability of the MnFe$_2$O$_4$/Au hybrid nanospheres modified GCE were also evaluated by conducting repetitive experiments for 20 times to detect 50 ppb As(III) on the modified electrode under the optimized conditions. Figure 6 shows the stripping current was nearly constant after continuous cycling for 20 times, and no obvious changes in the

peak currents were observed with the RSD of 1.9%. The good reproducibility, long-term stability, and favorable repeatability of $MnFe_2O_4$/Au hybrid nanospheres modified GCE make them attractive for the preparation of a electrochemical sensor toward As(III).
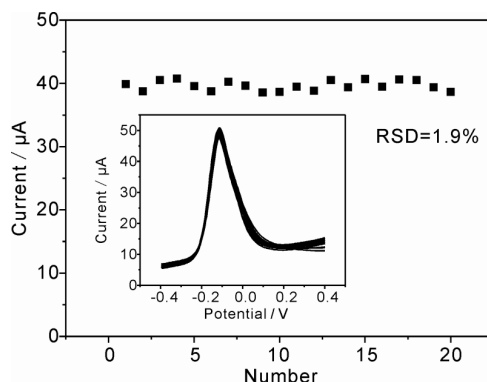

Figure 6. Repeatability measurements of 50 ppb As(III) on $MnFe_2O_4$/Au hybrid nanospheres modified GCE towards As(III) in 0.1 M HAc-NaAc (pH 5.0). Data are collected from every SWASV response shown in the inset. Experimental conditions are identical to those in Figure 4.

3.7. Real Sample Analysis

In order to evaluate the practical application of the $MnFe_2O_4$/Au hybrid nanospheres modified GCE, real water sample analyses were taken from laboratory tap water [26,42]. The real sample was diluted with a 0.1 M HAc-NaAc buffer solution (pH 5.0) in a ratio of 1:9 without any further treatment. The standard addition of 10 ppb As(III) was performed in the diluted sample and the recovery studies were carried out by further standard additions of As(III) into the diluted sample with a known concentration of As(III). The SWASV response and the corresponding calibration plot of peak currents against As(III) concentrations are presented in Figure 7. No obvious signals for As(III) were observed in the real samples (dash dotted line in Figure 7), indicating no As(III) was detected in the laboratory tap water. Furthermore, the recovery obtained is calculated to be 103% $\pm$ 8.1%, which reveals that the proposed detection method for As(III) has the potential for practical application.
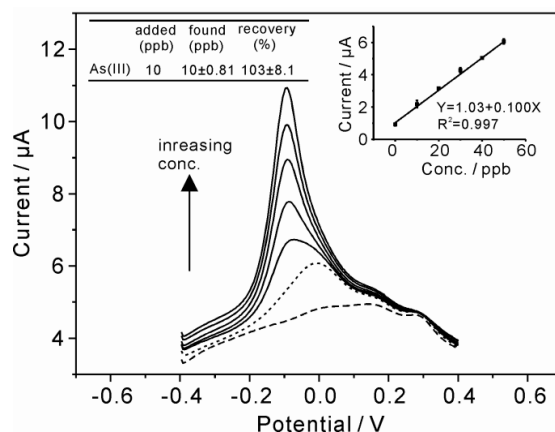

Figure 7. SWASV responses of standard additions of As(II) into a real water sample diluted with 0.1 M NaAc-HAc solution (pH 5.0) in a ratio of 1:9 and the corresponding calibration plot of peak current against As(II) concentrations. The dash dotted line is the baseline in the solution of 0.1 M NaAc-HAc (pH 5.0) containing 1.0 mL of the real sample. The dotted line is the SWASV response toward 10 ppb As(III) in the solution of 0.1 M NaAc-HAc (pH 5.0) containing 1.0 mL of the real sample. The inset table is the recovery calculation. Error bars are the standard deviation for three consecutive measurements. SWASV conditions are identical to those in Figure 4.

4. Conclusions

In summary, Au nanoparticles decorated mesoporous $MnFe_2O_4$ nanocrystal clusters ($MnFe_2O_4$/Au hybrid nanospheres) with high electrochemical performance were used for the electrochemical determination of As(III) by square wave anodic stripping voltammetry (SWASV). The as-prepared product was characterized by SEM, HRTEM, TEM, and EDS. The results suggest that 13 nm Au nanoparticles were indeed supported on the surface of mesoporous $MnFe_2O_4$ microspheres with the diameter of about 350 nm. Electrochemical behavior of the $MnFe_2O_4$/Au hybrid nanospheres modified GCE toward As(III) showed favorable sensitivity (0.315 μA/ppb) and LOD (3.37 ppb) for As(III) under the optimized conditions in 0.1 M NaAc-HAc (pH 5.0) by depositing for 150 s at the deposition potential of −0.9 V. No obvious interference from Cd(II) and Hg(II) was recognized during the detection of As(III). In addition, the excellent reproducibility, stability, and repeatability of $MnFe_2O_4$/Au hybrid nanospheres made it a promising electrode material for the electrochemical determination of As(III). Furthermore, the $MnFe_2O_4$/Au hybrid nanospheres modified GCE offered potential practical applicability in the electrochemical detection of As(III) in real water samples. Ultimately, the present work may provide a potential method for the design of new and cheap sensors in the application of electrochemical detection toward trace As(III) and other toxic metal ions.

Author Contributions: Shaofeng Zhou conceived and designed the experiments, analyzed the data, and completed the writing of the paper. Xiaojuan Han and Honglei Fan performed the experiments and analyzed the data. Yaqing Liu took part in the revising of the manuscript.

Conflicts of Interest: The authors declare no conflict of interest.

References

1. Mandal, B.K.; Suzuki, K.T. Arsenic round the world: A review. *Talanta* **2002**, *58*, 201–235. [CrossRef]
2. Jena, B.K.; Raj, C.R. Gold nanoelectrode ensembles for the simultaneous electrochemical detection of ultratrace arsenic, mercury, and copper. *Anal. Chem.* **2008**, *80*, 4836–4844. [CrossRef] [PubMed]
3. Dai, X.; Nekrassova, O.; Hyde, M.E.; Compton, R.G. Anodic stripping voltammetry of arsenic(III) using gold nanoparticle-modified electrodes. *Anal. Chem.* **2004**, *76*, 5924–5929. [CrossRef] [PubMed]
4. Li, D.; Li, J.; Jia, X.; Han, Y.; Wang, E. Electrochemical determination of arsenic(III) on mercaptoethylamine modified Au electrode in neutral media. *Anal. Chim. Acta* **2012**, *733*, 23–27. [CrossRef] [PubMed]
5. Mcgaw, E.A.; Swain, G.M. A comparison of boron-doped diamond thin-film and Hg-coated glassy carbon electrodes for anodic stripping voltammetric determination of heavy metal ions in aqueous media. *Anal. Chim. Acta* **2006**, *575*, 180–189. [CrossRef] [PubMed]
6. Wonsawat, W.; Dungchai, W.; Motomizu, S.; Chuanuwatanakul, S.; Chailapakul, O. Highly Sensitive Determination of Cadmium and Lead Using a Low-cost Electrochemical Flow-through Cell Based on a Carbon Paste Electrode. *Anal. Sci.* **2012**, *28*, 141–146. [CrossRef] [PubMed]
7. Liu, Z.G.; Huang, X.J. Voltammetric determination of inorganic arsenic. *Trend Anal. Chem.* **2014**, *60*, 25–35. [CrossRef]
8. Luong, J.H.T.; Lam, E.; Male, K.B. Recent advances in electrochemical detection of arsenic in drinking and ground waters. *Anal. Methods* **2014**, *6*, 6157–6169. [CrossRef]
9. Munoz, E.; Palmero, S. Analysis and speciation of arsenic by stripping potentiometry: A review. *Talanta* **2005**, *65*, 613–620. [CrossRef] [PubMed]
10. Zhang, Q.X.; Yin, L.B. Electrochemical performance of heterostructured Au-Pd bimetallic nanoparticles toward As(III) aqueous media. *Electrochem. Commun.* **2012**, *22*, 57–60. [CrossRef]
11. Simm, A.O.; Banks, C.E.; Compton, R.G. Sonically assisted electroanalytical detection of ultratrace arsenic. *Anal. Chem.* **2004**, *76*, 5051–5055. [CrossRef] [PubMed]
12. Kopanica, M.; Novotny, L. Determination of traces of arsenic(III) by anodic stripping voltammetry in solutions, natural waters and biological material. *Anal. Chim. Acta* **1998**, *368*, 211–218. [CrossRef]

13. Majid, E.; Hrapovic, S.; Liu, Y.L.; Male, K.B.; Luong, J.H.T. Electrochemical determination of arsenite using a gold nanoparticle modified glassy carbon electrode and flow analysis. *Anal. Chem.* **2006**, *78*, 762–769. [CrossRef] [PubMed]

14. Dai, X.; Wildgoose, G.G.; Salter, C.; Crossley, A.; Compton, R.G. Electroanalysis using macro-, micro-, and nanochemical architectures on electrode surfaces. Bulk surface modification of glassy carbon microspheres with gold nanoparticles and their electrical wiring using carbon nanotubes. *Anal. Chem.* **2006**, *78*, 6102–6108. [CrossRef] [PubMed]

15. Rassaei, L.; Sillanpaeae, M.; French, R.W.; Compton, R.G.; Marken, F. Arsenite determination in phosphate media at electroaggregated gold nanoparticle deposits. *Electroanalysis* **2008**, *20*, 1286–1292. [CrossRef]

16. Zakharova, E.A.; Noskova, G.N.; Kabakaev, A.S.; Rees, N.V.; Compton, R.G. Gold microelectrode ensembles: cheap, reusable and stable electrodes for the determination of arsenic (V) under aerobic conditions. *Int. J. Environ. Anal. Chem.* **2013**, *93*, 1105–1115. [CrossRef]

17. Salimi, A.; Manikhezri, H.; Hallaj, R.; Soltanian, S. Electrochemical detection of trace amount of arsenic(III) at glassy carbon electrode modified with cobalt oxide nanoparticles. *Sens. Actuators B Chem.* **2008**, *129*, 246–254. [CrossRef]

18. Gao, C.; Yu, X.Y.; Xiong, S.Q.; Liu, J.H.; Huang, X.J. Electrochemical detection of arsenic(III) completely free from noble metal: Fe_3O_4 microspheres-room temperature ionic liquid composite showing better performance than gold. *Anal. Chem.* **2013**, *85*, 2673–2680. [CrossRef] [PubMed]

19. Chen, X.; Liu, Z.G.; Zhao, Z.Q.; Liu, J.H.; Huang, X.J. SnO_2 tube-in-tube nanostructures: Cu@C nanocable templated synthesis and their mutual interferences between heavy metal ions revealed by stripping voltammetry. *Small* **2013**, *9*, 2233–2239. [CrossRef] [PubMed]

20. Yavuz, C.T.; Mayo, J.T.; Yu, W.W.; Prakash, A.; Falkner, J.C.; Yean, S.; Cong, L.L.; Shipley, H.J.; Kan, A.; Tomson, M.; *et al.* Low-field magnetic separation of monodisperse Fe_3O_4 nanocrystals. *Science* **2006**, *314*, 964–967. [CrossRef] [PubMed]

21. Wu, K.; Liu, T.; Xue, W.; Wang, X.C. Arsenic(III) oxidation/adsorption behaviors on a new bimetal adsorbent of Mn-oxide-doped Al oxide. *Chem. Eng. J.* **2012**, *192*, 343–349. [CrossRef]

22. Zhang, G.S.; Qu, J.H.; Liu, H.J.; Liu, R.P.; Wu, R.C. Preparation and evaluation of a novel Fe-Mn binary oxide adsorbent for effective arsenite removal. *Water Res.* **2007**, *41*, 1921–1928. [CrossRef] [PubMed]

23. Gupta, K.; Maity, A.; Ghosh, U.C. Manganese associated nanoparticles agglomerate of iron(III) oxide: Synthesis, characterization and arsenic(III) sorption behavior with mechanism. *J. Hazard. Mater.* **2010**, *184*, 832–842. [CrossRef] [PubMed]

24. Xu, W.H.; Wang, L.; Wang, J.; Sheng, G.P.; Liu, J.H.; Yu, H.Q.; Huang, X.J. Superparamagnetic mesoporous ferrite nanocrystal clusters for efficient removal of arsenite from water. *Crystengcomm* **2013**, *15*, 7895–7903. [CrossRef]

25. Zhou, S.F.; Han, X.J.; Fan, H.L.; Zhang, Q.X.; Liu, Y.Q. Electrochemical detection of As(III) through mesoporous $MnFe_2O_4$ nanocrystal clusters by square wave stripping voltammetry. *Electrochim. Acta* **2015**, *174*, 1160–1166. [CrossRef]

26. Wu, S.G.; Zhao, Q.P.; Zhou, L.; Zhang, Z.X. Stripping analysis of trace arsenic based on the MnOx/AuNPs composite film modified electrode in alkaline media. *Electroanalysis* **2014**, *26*, 1840–1849. [CrossRef]

27. Cui, H.; Yang, W.Y.; Li, X.J.; Zhao, H.; Yuan, Z.B. An electrochemical sensor based on a magnetic Fe_3O_4 nanoparticles and gold nanoparticles modified electrode for sensitive determination of trace amounts of arsenic(III). *Anal. Methods* **2012**, *4*, 4176–4181. [CrossRef]

28. Deng, H.; Li, X.; Peng, Q.; Wang, X.; Chen, J.; Li, Y. Monodisperse magnetic single-crystal ferrite microspheres. *Angew. Chem.* **2005**, *117*, 2842–2845. [CrossRef]

29. Guo, S.; Dong, S.; Wang, E. A general route to construct diverse multifunctional Fe_3O_4/metal hybrid nanostructures. *Chemistry* **2009**, *15*, 2416–2424. [CrossRef] [PubMed]

30. Guo, S.; Dong, S.J.; Wang, E. Constructing carbon-nanotube/metal hybrid nanostructures using homogeneous TiO_2 as a spacer. *Small* **2008**, *4*, 1133–1138. [CrossRef] [PubMed]

31. Liu, J.; Sun, Z.K.; Deng, Y.H.; Zou, Y.; Li, C.Y.; Guo, X.H.; Xiong, L.Q.; Gao, Y.; Li, F.Y.; Zhao, D.Y. Highly water-dispersible biocompatible magnetite particles with low cytotoxicity stabilized by citrate groups. *Angew. Chem. Int. Ed.* **2009**, *48*, 5875–5879. [CrossRef] [PubMed]

32. Wu, N.; Wei, H.H.; Zhang, L.Z. Efficient removal of heavy metal ions with biopolymer template synthesized mesoporous titania beads of hundreds of micrometers size. *Environ. Sci. Technol.* **2012**, *46*, 419–425. [CrossRef] [PubMed]

33. Zhu, T.; Chen, J.S.; Lou, X.W. Highly efficient removal of organic dyes from waste water using hierarchical NiO spheres with high surface area. *J. Phys. Chem. C* **2012**, *116*, 6873–6878. [CrossRef]

34. Ge, J.P.; Hu, Y.X.; Biasini, M.; Beyermann, W.P.; Yin, Y.D. Superparamagnetic magnetite colloidal nanocrystal clusters. *Angew. Chem. Int. Ed.* **2007**, *46*, 4342–4345. [CrossRef] [PubMed]

35. Wang, X.F.; You, Z.; Sha, H.L.; Sun, Z.L.; Sun, W. Electrochemical myoglobin biosensor based on carbon ionic liquid electrode modified with $Fe_3O_4@SiO_2$ microsphere. *J. Solid State Electr.* **2014**, *18*, 207–213. [CrossRef]

36. Hung, D.Q.; Nekrassova, O.; Compton, R.G. Analytical methods for inorganic arsenic in water: A review. *Talanta* **2004**, *64*, 269–277. [CrossRef] [PubMed]

37. Wei, Y.; Yang, R.; Liu, J.H.; Huang, X.J. Selective detection toward Hg(II) and Pb(II) using polypyrrole/carbonaceous nanospheres modified screen-printed electrode. *Electrochim. Acta* **2013**, *105*, 218–223. [CrossRef]

38. Feeney, R.; Kounaves, S.P. On-Site Analysis of arsenic in groundwater using a microfabricated gold ultramicroelectrode array. *Anal. Chem.* **2000**, *72*, 2222–2228. [CrossRef] [PubMed]

39. Zen, J.M.; Liou, S.L.; Kumar, A.S.; Hsia, M.S. An efficient and selective photocatalytic system for the oxidation of sulfides to sulfoxides. *Angew. Chem. Int. Ed.* **2003**, *42*, 577–599. [CrossRef] [PubMed]

40. Simm, A.O.; Banks, C.E.; Wilkins, S.J.; Karousos, N.G.; Davis, J.; Compton, R.G. A comparison of different types of gold-carbon composite electrode for detection of arsenic(III). *Anal. Bioanal. Chem.* **2005**, *381*, 979–985. [CrossRef] [PubMed]

41. Profumo, A.; Fagnoni, M.; Merli, D.; Quartarone, E.; Protti, S.; Dondi, D.; Albini, A. Multiwalled carbon nanotube chemically modified gold electrode for inorganic as speciation and Bi(III) determination. *Anal. Chem.* **2006**, *78*, 4194–4199. [CrossRef] [PubMed]

42. Li, W.J.; Yao, X.Z.; Guo, Z.; Liu, J.H.; Huang, X.J. Fe_3O_4 with novel nanoplate-stacked structure: Surfactant-free hydrothermal synthesis and application in detection of heavy metal ions. *J. Electroanal. Chem.* **2015**, *749*, 75–82. [CrossRef]